Impulse Force Calibration:

Design and Simulation of a New Calibration Device

Thomas Bruns, Michael Kobusch
Physikalisch-Technische Bundesanstalt (PTB), Braunschweig, Germany

Abstract

In addition to the dynamic force calibration with harmonic excitation, a new method for impulse forces is under development at PTB in Braunschweig. The forces of up to 20 kN are generated by the impact of two masses guided by air bearings. Traceability for force is realized via the measurement of acceleration with laser-Doppler-interferometers and the determination of the moving masses.

1. Design of the Calibration Device

A new calibration device at PTB is supposed to provide traceability for impulse forces up to 20 kN via the SI units of mass and acceleration (as the ratio velocity over time). Force is generated in the device by the central collinear impact of two bodies, which are guided in individual air bearings. The transducer under calibration is mounted on one of these masses facing the other. By measuring the velocities of these bodies against time, it is possible to calculate their acceleration and deceleration respectively and thus to calculate the force acting on the transducer.

This so-called mass impact module (MI) consists of two stainless steel bodies M_1 and M_2 with a mass of approximately 10 kg each. Linear air bearings are used to guide the masses during initial acceleration and impact. The air bearings will provide an air film of average thickness 15 µm with a stiffness of about 300 N/µm at a working pressure of $5 \cdot 10^5$ Pa. Air is supplied to the guide ways through 128 pockets of a porous sintered metal with an average pore diameter of 8 µm and a surface area of 400 mm^2 per pocket. A sectional view of a single air bearing is given in Fig. 1.

The force transducer to be calibrated is mounted on the front of M_2, which is initially at rest. M_1 is accelerated to the initial impact velocity by a spring-loaded bolt (cf. Fig. 2). The acceleration is such that the body still has some distance to go before impacting on the

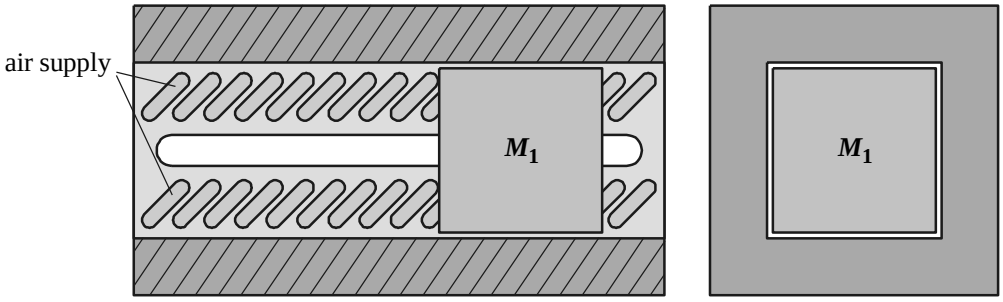

Figure 1. Profile (left) and cross-section (right) of one of the linear air bearings providing a view onto the guideway with its air-supply pockets and the slotted hole for LDI measurements.

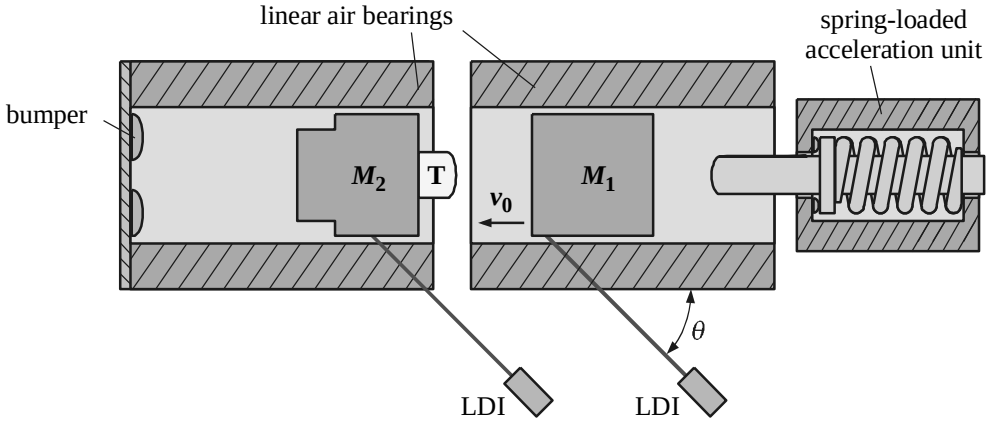

Figure 2. Setup of the mass impact module with linear air bearings, mass bodies M_1 and M_2, spring loaded acceleration unit and laser-Doppler-interferometer for velocity measurement.

transducer. Thus it is ensured that there is no coupling between bolt and transducer at any time during the measurement.

The effective velocity of the masses is measured by laser-Doppler-interferometry (LDI) performed on the lateral sides of M_1 or M_2 respectively. The special geometry of the measuring laser beam requires a retro-reflection under oblique incidence, which is achieved by retro reflective micro balls of highly refractive glass, fixed on the surface.

2. Simulation

In a first approximation the force F loaded onto the transducer is given by Newton's law

$$F(t) = m \cdot a(t) = m \cdot \frac{\mathrm{d}v}{\mathrm{d}t} \qquad (1)$$

As the product of mass m and acceleration a which in turn is the derivative of the velocity v over time t.

This equation can be applied to the measurement with the MI as long as the assumptions hold, of M_1 and M_2 being rigid bodies, and the coupling of the bodies to the transducer also being rigid. However, these assumptions al-

ready failed in some investigations in the field of harmonic force calibration [1]. This means that instead of equation (1) an integrated force has to be considered, i. e.

$$F(t) = \int_V \rho \cdot a(\boldsymbol{x},t) \cdot \mathrm{d}V \quad . \tag{2}$$

Here, V is the volume of the body whose acceleration is under examination and the vector $\boldsymbol{x}$ defines the location in the body. With the reasonable assumption of incompressibility the mass density ρ is constant which leads to

$$\begin{aligned} F(t) &= \rho \int_V a(\boldsymbol{x},t) \cdot \mathrm{d}V \\ &= m \cdot \frac{\int a(\boldsymbol{x},t) \cdot \mathrm{d}V}{V} \\ &= m \cdot \bar{a}(t) \end{aligned} \tag{3}$$

Which can be considered as a definition of the mean acceleration $\bar{a}(t)$.

Since LDI measurements only reveal data from the surface of a body, its total acceleration distribution a ($\boldsymbol{x}$, t) is accessible by modelling only. The proposed method to estimate the deviation of the integrated distribution $\bar{a}(t)$ from the measured value at the surface is the finite element (FEM) simulation. Here the integral of the volume is discredited using a 3D-mesh and the continuous distribution a ($\boldsymbol{x}$,t) becomes a series of $a_i(t)$ such that equation (3) changes to

$$\begin{aligned} F(t) &= m \cdot \frac{\sum_i a_i(t) \cdot \Delta V_i}{V} \\ &= m \cdot \bar{a}(t) \end{aligned} \tag{4}$$

Where the index i covers all nodes of the FEM-mesh of the formerly considered volume V.

In order to estimate the deviation of the force determined by LDI measurements on the surface and the 'true' force evaluated by a volume integration of the total acceleration distribution, the simulation result $a_s(t)$ at one appropriate surface node of the FEM-mesh was compared to $\bar{a}(t)$ of equation (4).

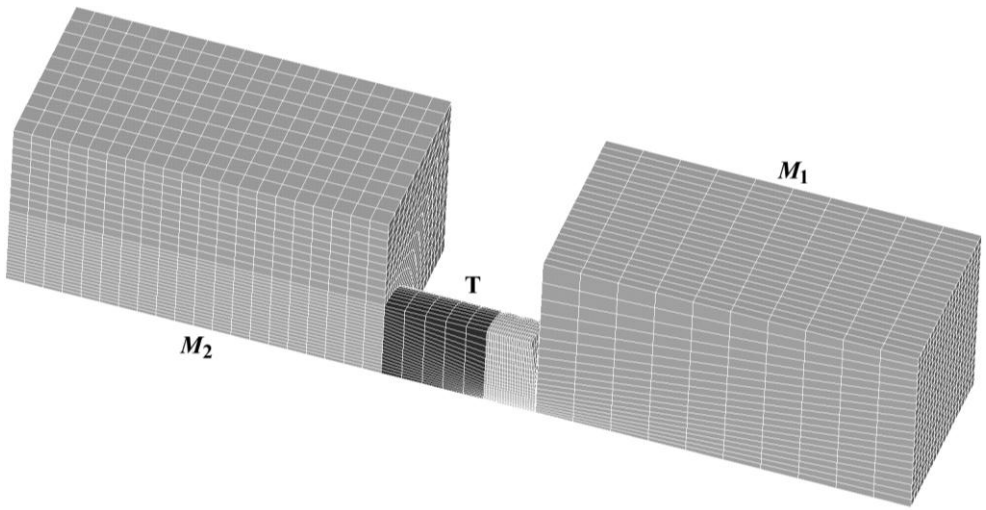

Figure 3. Quarter section of the FEM-model used to calculate the deviation between the LDI-derived force and the force calculated with the volume integrated acceleration distribution.

The FEM-model which was used for the simulation consists of two cube-shaped masses made of steel and a cylindrical transducer which has a convex steel-cap in the direction of M_1 and a elastic cylindrical body coupled to M_2. The modulus of elasticity of the latter was chosen to give an axial compression of 0,3 mm at a static load of 20 kN in order to represent the characteristics of a typical strain-gage transducer. A quarter section of the FEM-mesh is shown in Fig. 3.

Results of the simulation are displayed in the following figures. The simulated sampling rate was 500 kHz. However, in order to suppress the intrinsic high frequency oscillations of the FEM-mesh, which are due to the numerical algorithm, the calculated velocity data were subsequently filtered using a running average FIR-filter with a Henning window of 41 samples width. This reduces the effective frequency range to approximately 20 kHz.

The resulting force signal consists of two phases. The impact, which happens approximately between 0,2 ms and 1,3 ms, and a subsequent oscillation of the transducer's steel cap and parts of its elastic body against M_2.

To calculate the deviation between the volume acceleration $\bar{a}(t)$ described by equation (4) and the surface acceleration $a_s(t)$, a χ^2-fit of the form $\sum_j (\bar{a}_j - b_a \cdot a_{s,j})^2 = \min.$ was performed (cf. Fig. 4). Here, j denotes the

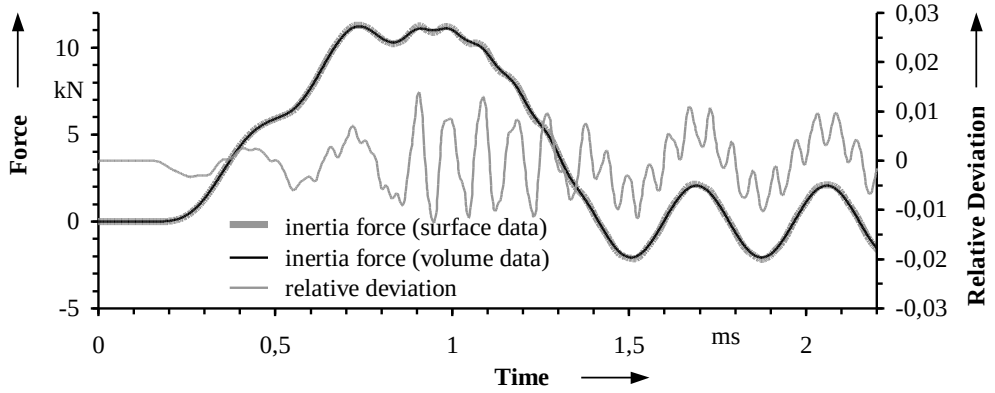

Figure 4. Comparison of inertia forces calculated from the volume acceleration $\bar{a}(t)$ and the surface acceleration $a_s(t)$ and their relative deviation normalized to the maximum force.

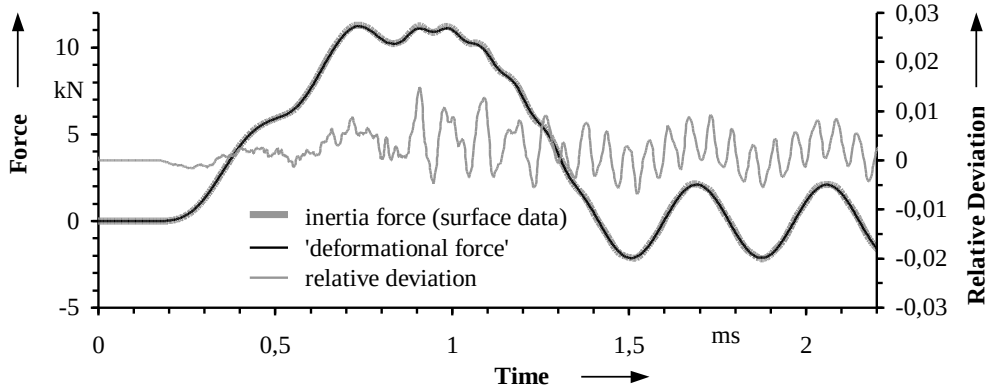

Figure 5. Comparison of 'deformational force' $b_f \cdot S \cdot \Delta u(t)$ and inertia force $m \cdot a_s(t)$ calculated from the surface acceleration a_s and their relative deviation normalized to the maximum force.

number of the time step. This fit resulted in b_a = 0,9989 which indicates that, as regards the accuracy of the FEM-model, the non-rigidity of the steel masses can be neglected.

In order to test the concept of traceability for the device, an analogous fit was performed between the 'deformational force', which was calculated from the axial compression $\Delta u(t)$ of the elastic body of the transducer times its stiffness S, versus the 'measured force' calculated as $m \cdot a_s(t)$. In this case the formula $\sum_j (m \cdot a_{s,j} - b_f \cdot S \cdot \Delta u_j)^2 = \min.$ was used. The fit parameter was calculated to b_f = 1,0044 which is again of the order of accuracy of the chosen numerical algorithm (cf. Fig. 5).

In addition to the different force signals, their relative deviations over time are displayed. The deviations show high frequency components, which are dependent on the filter characteristics. With the filter described above the maximum relative deviation between the 'measured force' $m \cdot a_s(t)$ and the 'deformational force' $b_f \cdot S \cdot \Delta u(t)$, as well as between the surface acceleration $a_s(t)$ and the volume acceleration $\bar{a}(t)$, or their respective forces, is less than 2 %.

3. Preliminary Tests of the Optical Measurement Instrumentation

The traceability of impact force measurements requires an accurate determination of the impacting bodies' acceleration, which will be derived from an LDI velocity signal capable of being calibrated to a satisfying uncertainty of the order of 10^{-3}. Of course, appropriate signal filtering techniques have to be utilized in order to suppress signal noise, which is strongly amplified by the differentiation process itself. Further difficulties may arise from the oblique incidence of the measuring laser beam, which sweeps over the target surface due to its transverse velocity component.

Preliminary tests of impact force measurements were carried out in order to prove the concept of measurement instrumentation, which is planned for the MI. For this purpose a piezoelectric force transducer of 20 kN nominal load was mounted on a modified pendulum impact tester (length of pendulum ca. 0,25 m) formerly used in the field of materials testing. Here, pulse forces were generated by the hammer's moving mass (≈0,65 kg) impacting on the rigidly mounted transducer. With different types of thin elastic pads inserted between the colliding bodies, pulses of various duration were achieved. A sketch of this experimental set-up is shown in Fig. 6.

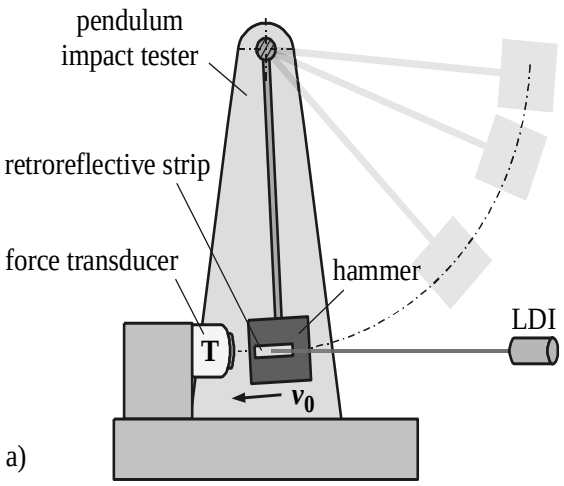

a)

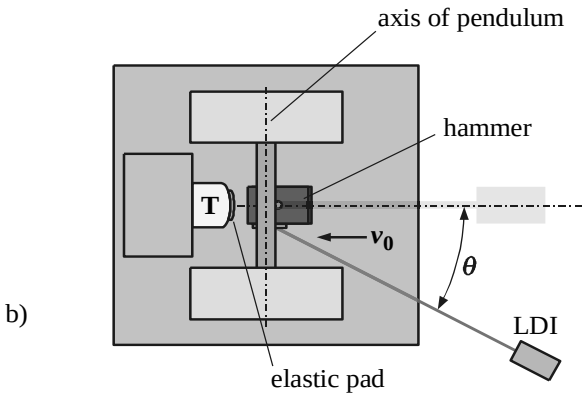

Figure 6. Pendulum impact tester with mounted force sensor T and LDI instrumentation: side view (a), top view (b)

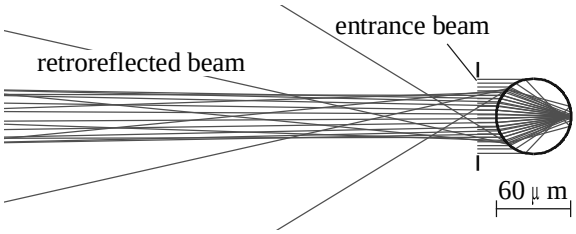

Figure 7. Retro reflection of a high index glass ball. For sake of clarity, the collimated entrance beam is omitted in the far field at left.

The velocity v_0 of the impacting hammer was measured by a fibber LDI (Polytec Vibrometer OFV 512) aimed at its lateral side under an oblique angle. The measuring laser beam and the velocity vector were inclined at an angle of θ=40° and thus the corresponding line of sight velocity component $v_0 \cdot \cos\theta$ was measured.

To achieve sufficient intensity of the surface-reflected interferometer beam, a strip of retro reflective adhesive sheeting was applied to the surface. This special sheeting contains tiny micro spheres of high index glass (n≈1,9) with an average diameter of about 60 µm, which act as individual retro reflectors.

Collimated light that enters into such a glass ball is focused and internally reflected in such a way that a backward directed exit beam of good collimation is obtained (cf. Fig. 7). Furthermore, the rear-side of the micro spheres is metallized in order to gain high reflectivity.

Under dynamic excitation a minor relative motion between the surface and its retro reflector, which might affect LDI, velocity data generally cannot be ruled out. Compared to rigidly bonded glass beads the elastic fixing of relatively thick adhesive sheeting could be problematic. Although impacting occurs just within a fraction of a millimeter, the transverse motion of the surface can cause intensity fluctuations, which lead to a poorer signal quality. Regarding these aspects further tests are necessary and will be published later.

Figure 8 gives two examples of impact force measurements with pulses of different duration and amplitude where the measured piezoelectric force signal is compared to the corresponding signal derived from LDI velocity data. All data acquisition was accomplished by a transient recorder (Nicolet Odyssey) at 14 bit resolution and 100 kHz sampling rate.

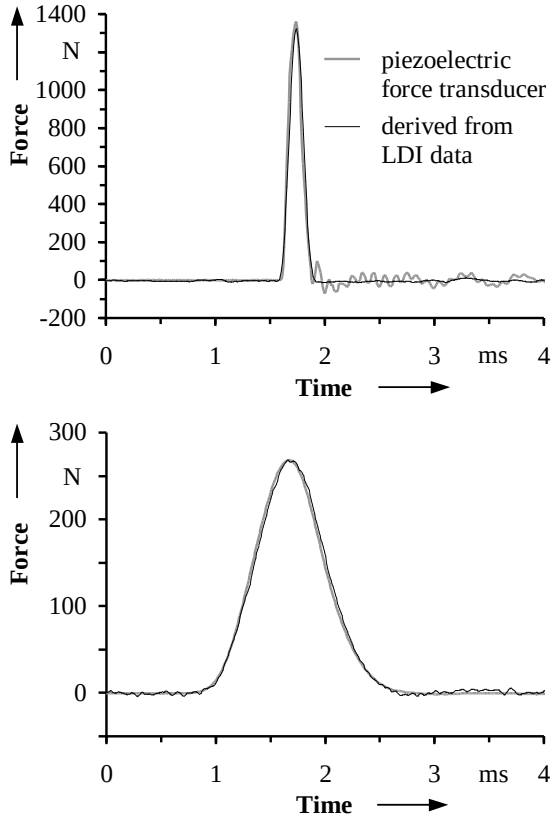

Figure 8. Comparison of measured impact pulses of about 0,3 ms and 1,8 ms duration.

The diagrams demonstrate that the general pulse shape of both signals is in very good agreement. Post-impact oscillations of the piezoelectric force transducer, similar to those earlier modelled by FEM, can be discerned in the signal of the 0,3 ms pulse. Moreover, it is obvious that the measured pulse shapes deviate from the typical half-sine characteristic of a linear model due to non-linear contact forces.

4. Conclusion

This paper describes a new impulse force calibration facility, which is now under construction at PTB. The traceability of impact forces generated by a collinear collision of two heavy masses guided by air bearings will make use of LDI velocity measurements obtained at the surfaces. FEM simulations show that the volume integrated inertia force generated in that body, which is initially at rest, can be picked up at its surface without introducing significant errors. Additionally, good agreement between the inertia force of the accelerated mass and the elastic deformation, which would be sensed by the modelled force transducer, was calculated. It is shown further; that preliminary tests obtained at a pendulum impact tester proved that LDI measurements under oblique incidence are appropriate for use on the mass impact module later.

5. References

[1]. Kumme R., Peters M., Sawla A., *Improvements of Dynamic Force Calibration Part II*, Final Report, bcr information Applied Metrology, European Commission, Luxembourg, 1995.

Contact Person for Paper:

Dr. Thomas Bruns
Address:
Physikalisch-Technische Bundesanstalt,
Fachlabor 1.13,
Bundesallee 100, 38116 Braunschweig,
GERMANY,
Fax: +49 531 592 1105,
Tel: +49 531 592 1132

e-mail: thomas.bruns@ptb.de